EFFECTS OF MICROSCALE WIND DISTURBANCE ON EVTOL AIRCRAFT PERFORMANCE DURING LANDING

Nithya D S
PhD Student
Politecnico di Milano
RMIT University
Milan, Italy

Agata Rylko
PhD Student
Politecnico di Milano
Milan, Italy

Vincenzo Muscarello
Senior Lecturer
RMIT University
Melbourne, Australia

Man Liang
Senior Lecturer
RMIT University
Melbourne, Australia

Giuseppe Quaranta
Full Professor
Politecnico di Milano
Milan, Italy

ABSTRACT

The primary conception of Urban Air Mobility is to transport people and goods within cities by operating electric Vertical Take-Off and Landing aircraft at low altitudes where microscale wind conditions are pervasive. These wind disturbances within the urban canopy pose several challenges to near-ground flight phases and one such risk is the possibility of landing trajectory deviation. This paper investigates the effects of wind on an eVTOL landing performance and its corresponding trajectory by integrating microscale wind velocity field data into a flight simulator. Initially, a reference trajectory is generated to depict a scenario of an eVTOL landing on the ground, at the leeward side of a building, for no wind conditions. Then, the microscale wind data representing the flow over an isolated building are synthesized and introduced into the flight simulator to update the landing trajectory in the presence of wind disturbance for assessing the wind-induced aircraft performance deviations.

INTRODUCTION

Urban Air Mobility (UAM) vehicles such as electric Vertical Take-Off and Landing aircraft (eVTOLs) are susceptible to the prevailing microscale wind disturbances in congested low-altitude urban airspace. This would introduce safety concerns like trajectory deviation, which may lead to collision risks when flying. The consequences and severity of such threats would be especially pronounced for near-ground flight phases such as takeoff and landing due to the proximity of the building structures. However, many existing studies focus only on generating wind-optimal trajectories and developing robust controllers for eVTOL drones by factoring mesoscale wind data, Dryden or Von Kármán gusts as wind uncertainties (Refs. 1,2).

For instance, in (Ref. 3), researchers from NASA investigate the probability of trajectory deviation of an octocopter using steady-state interpolated forecast data and turbulent (Von Kármán) wind conditions in a low-fidelity flight dynamics model, that represents the octocopter or eVTOL as a sphere with beams and ignores the intricacies of rotor aerodynamics. The study focuses only on assessing the flight path variation at turn waypoints for different airspeeds, neglecting the landing trajectory. Likewise, Taymourtash et al. (Refs. 4–7) have conducted a series of wind tunnel test campaigns to replicate a helicopter landing on a ship deck. However, the study has been primarily aimed at investigating the aerodynamic interactions between ship air wake and the rotor response. Bath et al. (Ref. 8) analyze the effects of three different low-altitude turbulence intensities on the rotor speed response of a quadcopter to determine the actuator effort required for disturbance rejection. Along similar lines, Siqueira (Ref. 9) investigates the effects of wind on the trajectory of a fixed-wing UAV. But, the study utilizes a wind model reflective of a velocity spectrum based on the Dryden turbulence model for an altitude less than 2000ft rather than a microscale wind model.

On the whole, it is evident that a research gap persists in employing microscale wind models or data for inspecting the effects of low-altitude atmospheric conditions on UAM aircraft and operations. Therefore, the primary objective of this paper is to study the effects of a simulated microscale wind disturbance on the trajectory of an eVTOL drone landing behind an isolated building. The overall approach encompasses the development of a test scenario and integration of a custom wind database to a flight simulator as depicted in Fig. 1 for aircraft performance analysis. This methodology would be relevant for both the design of aircraft and Vertiports, as well as for the certification of Unmanned Aircraft Systems with a Specific Assurance and Integrity Level (SAIL) higher than IV or aircraft requiring specific design verification processes, or eVTOLs that must adhere to the Special Condition VTOL standards (see (Refs. 10–12).

The microscale wind model used for this study is developed with the help of multiple open-source software as listed below.

1. A steady-state microscale wind simulator, *QES-Winds* (Ref. 13).
2. An inflow turbulence simulator, *TurbSim* (Ref. 14).
3. An inflow wind data processing software, *InflowWind* (Ref. 15).

QES-Winds is a diagnostic wind simulator that generates high-resolution 3D time-averaged wind flow field vectors $(\bar{u}(x,y,z), \bar{v}(x,y,z), \bar{w}(x,y,z))$ based on just the principles of mass conservation. Although the software is primarily intended for rapidly estimating pollution dispersion, highly parameterized wind simulators such as QES-Winds can be explored for employment within the UAM sector due to their higher computational efficiency (Ref. 16). However, utilizing QES-Winds as a standalone data generator would be insufficient to represent or simulate the turbulent atmospheric wind conditions within the Urban Boundary Layer (UBL). Hence, a stochastic turbulence simulator, TurbSim is used along with QES-Winds. As a result, the wind data generated by QES-Winds in the inertial reference frame is post-processed to identify the mean wind profile of a specific 2D (YZ) plane behind the building and used as an input for the TurbSim simulation. TurbSim, then, synthesizes the turbulent time series data of the 3 wind velocity components $(u(y,z,t), v(y,z,t), w(y,z,t))$.

Albeit the ability of TurbSim to produce full-field turbulent inflow wind data, it can only simulate turbulence for a fixed 2D (YZ) rectangular domain (Ref. 14). Thus, to obtain turbulent wind velocity field data for a 3D domain, an additional software module called InflowWind is exercised. InflowWind makes use of Taylor's frozen hypothesis to propagate the TurbSim output in space (X-direction) and time to produce the 3 component turbulent wind velocity vectors $(u(x,y,z,t), v(x,y,z,t), w(x,y,z,t))$ for a 3D simulation domain in the inertial reference frame. The resultant velocity vector derived from InflowWind is stored in a database and later integrated into a flight simulator.

The flight simulator used for this study is representative of a lift+cruise eVTOL drone (see Figure 2) with a mass of 7.1 kg and a wingspan of 3.12 m. It is built and facilitated by graduate student researchers at the Aerospace Systems and Controls Laboratory (ASCL) of Politecnico di Milano, Italy. The flight dynamics unit in the simulator symbolizes the dynamics of a rigid-body aircraft using non-linear equations of motion and the quasi-linear parameter varying (qLPV) model which constructs the aerodynamic data altering with the airspeed. Furthermore, the simulator embodies two types of controllers: one for multicopter and one for fixed-wing configuration. For this study, the multicopter controller which employs a conventional PID cascaded loops architecture is used to maintain a constant altitude and level attitude. For more details on the features of the simulator, the interested reader is referred to Refs. 17–20

The following sections describe the test scenario, the steps in creating and integrating the microscale wind database into the flight simulator, the flight simulation, and the corresponding results and analysis. Lastly, the paper concludes with a summary of the findings and recommendations for future work.

MICROSCALE WIND SIMULATION

As a first step, a test scenario is assumed depicting an eVTOL landing on the ground behind a building (20x20x40 m) with a constant reference landing speed, V_{ref}, of 1 m/s from an altitude of 40 m. QES-Winds uses this information to simulate the steady-state wind, but it is not sufficient to set the domain for the TurbSim and InflowWind simulations. Hence, exploiting the Means of Compliance Special condition VTOL guidelines (Ref. 21) and considering the current eVTOL wingspan, the Final Approach and Take-Off (FATO) zone and the Safety Area (SA) are assumed to have a 12m and 15m diameter, respectively, with a landing point positioned at the center (that is, 15 m from the rear of the building). Based on the placement of FATO and SA on the leeward side of the building, the TurbSim plane is assumed to be at 7m ahead of the center of the FATO, while the InflowWind domain is considered to cover the entire FATO and SA as shown in Figure 3.

After the identification of the simulation domain, the steady-state wind simulation is carried out using QES-Winds for the input parameters listed in Table 1.

Table 1. QES-Winds simulation input parameters

Inputs	Value	Units
Domain	200x200x200	m
Mesh resolution	1x1x1	m
Initial wind speed	5	m/s
Initial wind direction	270	degrees
Inlet velocity profile	Log law	-

The steady-state wind data obtained from QES-Winds are processed to identify the flow field around the building. QES results show (see Fig. 4) that a stagnation point is predicted at $z/h = 0.75$ where the flow reverses to create a vortex in the upwind region of the building. Likewise, a recirculation zone is formed at the leeward side stretching up to 30 m downwind from the building. This indicates that the assumed FATO and SA are entirely within the leeside vortex zone.

The mean velocity profile in the YZ plane at 7 meters behind the building is identified and used as a reference wind profile for the TurbSim turbulence simulator. It can be noted from Fig. 5 that the velocity magnitude of the wind is less than 1.5 m/s within the recirculation zone (up to 30 m above the ground).

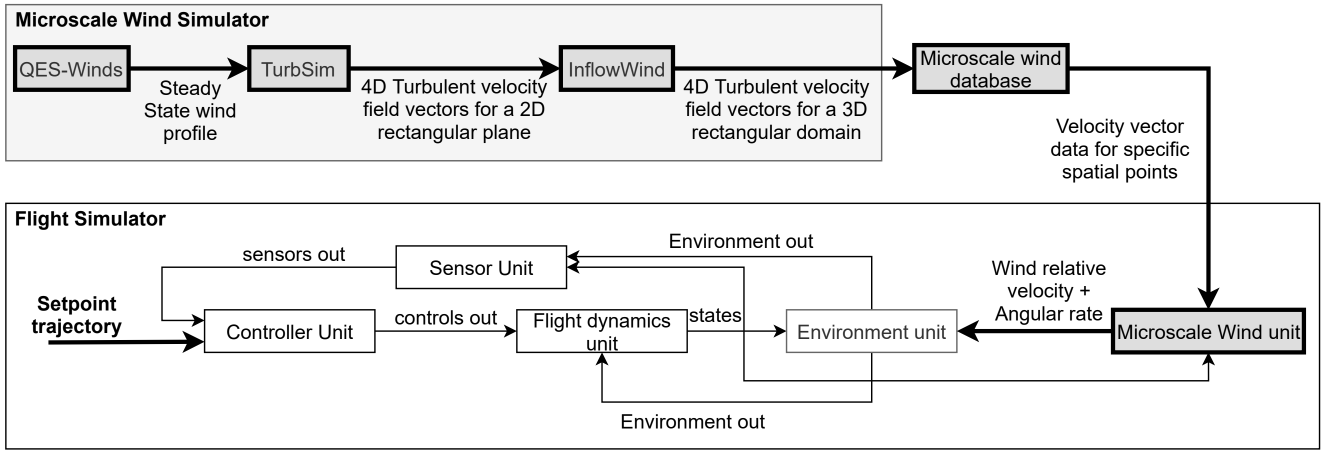

Figure 1. Flowchart of the overall methodology.

Figure 2. Lift+Cruise eVTOL drone aircraft in the lab (Ref. 17).

The input parameters utilized in the TurbSim inflow turbulence generator are listed in Table 2. It must be remarked that the current simulation is slated to produce a turbulence spectrum dictated by the Kaimal model, which is widely recognized and regulated within the Wind Engineering domain for representing low-altitude wind conditions. The Kaimal model was chosen over the aviation industry standardized Von Kármán or Dryden turbulence models, as the latter are primarily used for high-altitude turbulence representation.

Table 2. TurbSim simulation input parameters.

Inputs	Value	Units
Domain	21x39	m
Grid resolution	1x1	m
Initial wind speed	5	m/s
Initial wind direction	270 (clockwise)	degrees
Inlet velocity profile	QES mean wind profile	-
Timestep	0.05	s
Analysis time	600	s
Turbulence model	Kaimal model	-
Turbulence Intensity	High	-

As previously mentioned, the data obtained from TurbSim reflect the full field turbulent wind velocities of a fixed 2D rectangular plane (i.e., the YZ plane) in front of FATO or 7m behind the building, and this information is still not sufficient to characterize the wind velocities within the FATO zone. Consequently, to address the lack of details, the TurbSim output is used as an input within the InflowWind software module. The 3D InflowWind domain size is set to be 21x21x39 m with a grid resolution of 1x1x2 m for an analysis time of 90 s with 1s timestep to produce 3D turbulent wind velocity data (see Fig. 6) for the area covering the FATO and SA.

To check if the mean wind profile generated by TurbSim and InflowWind is similar to the inlet wind profile (i.e., the steady-state QES wind profile), the corresponding mean velocity data are calculated and shown in Fig. 7. It can be observed that the steady-state wind profile produced by QES and the time-averaged steady-state profile generated by TurbSim are quite similar. Whereas, the velocity profile yielded by InflowWind is rather overestimated within the vortex region. This could be due to the reduced grid resolution of InflowWind propagation in the vertical direction (2 m) compared to TurbSim and QES (1 m) simulation.

The time series data obtained from InflowWind correspond to both the steady-state wind components and fluctuations at each time step. Thus, for a deeper understanding, a spectral analysis is performed to determine the corresponding frequency content and the energy spectrum. The time series data of the turbulent velocities are converted into Power Spectral Densities using Welch's method for a window length equal to the total simulation time and a sample rate of 1Hz. As shown in Fig. 8, the velocity and kinetic energy spectra for different altitudes have a similar trend. The velocity spectra plot implies that there is a high frequency of lower wind velocity magnitudes at different altitudes. Whereas, the energy spectra for different altitudes suggest that the rate of dissipation of eddies is rapid and steep. The presence of larger eddies with an energy magnitude of 100 is lower when compared to the existence of the smaller eddies with a magnitude range between 0.1 and 0.01.

Finally, the turbulence intensity is calculated using Eq. 1 showing a maximum of 30.47% at about 25 m height (see

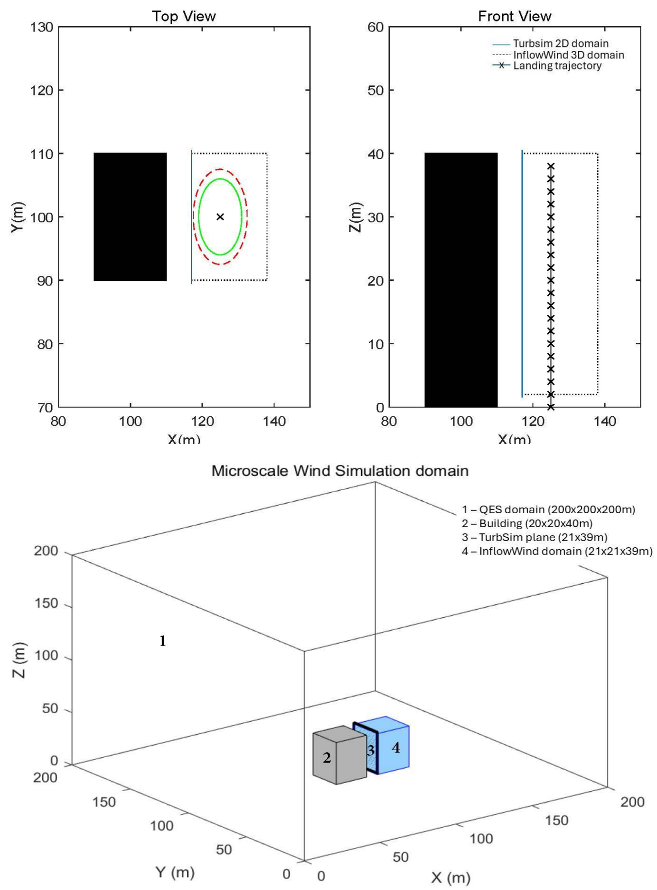

Figure 3. Picture showing the assumed FATO (area within the green circle), SA (area between the red and green circle), landing point ('x' marker in Top View), vertical landing trajectory, and the building (black rectangle).

Fig. 9).

$$TI = \frac{U_{rms}}{\bar{U}} \tag{1}$$

Subsequently, the generated microscale wind data is stored in a database for integration with the flight simulator. One of the main advantages of this type of wind modeling, compared to traditional wind models used in the aviation sector, is the ability to provide detailed knowledge of wind characteristics at a microscale level within the FATO area for a lower computational cost and time. Specifically, the computation time for QES simulation required 3.6 seconds on a NVIDIA GeForce RTX 9030 GPU, while TurbSim and InflowWind took approximately 50 and 4 seconds, respectively, on a CPU with a 11–th Gen Intel processor with 4 cores and a base speed of 2.80 GHz.

FLIGHT SIMULATION

The introduction of microscale wind data into the flight dynamics and environment unit of the flight simulator is performed by discretely querying the wind database at certain spatial points and time steps based on the setpoint trajectory

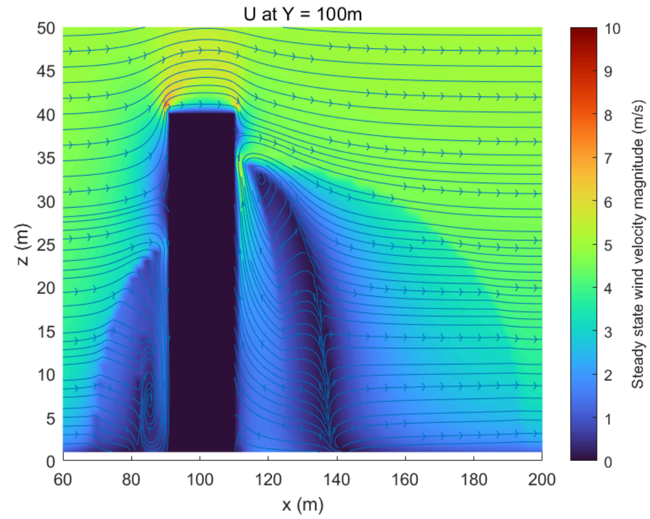

Figure 4. Steady state velocity magnitude change and streamlines over the building.

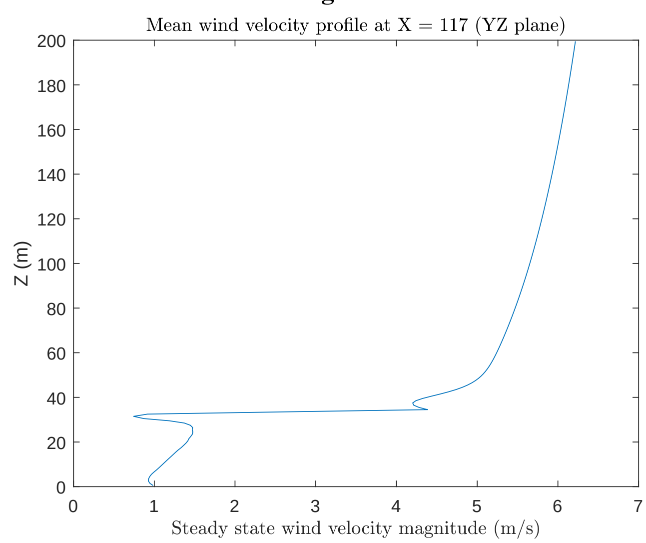

Figure 5. Wind profile infront of the FATO.

and flight time. Then, the queried data is rotated from the inertial reference frame to the body fixed frame using the following equation to obtain the relative wind velocity and the corresponding change in trajectory and flight response.

$$U_r = R_n^b(\phi_i, \theta_i, \psi_i) \begin{pmatrix} u(x_i, y_i, z_i, t_i) \\ v(x_i, y_i, z_i, t_i) \\ w(x_i, y_i, z_i, t_i) \end{pmatrix} \tag{2}$$

Initially, a setpoint trajectory illustrating a simple vertical takeoff, cruise and vertical landing is designed and injected into the simulator (see Fig. 10). The initial position of the aircraft is on the ground, while the trajectory setpoint is configured at 40 m above the ground in the east direction. The landing commences from a 40 m altitude above 1 m north. The flight speed and time are assigned to be 1 m/s and 90 s respectively, whereas the simulation time step is defined as 0.001 s.

Once the setpoint trajectory is set, the flight simulation is first

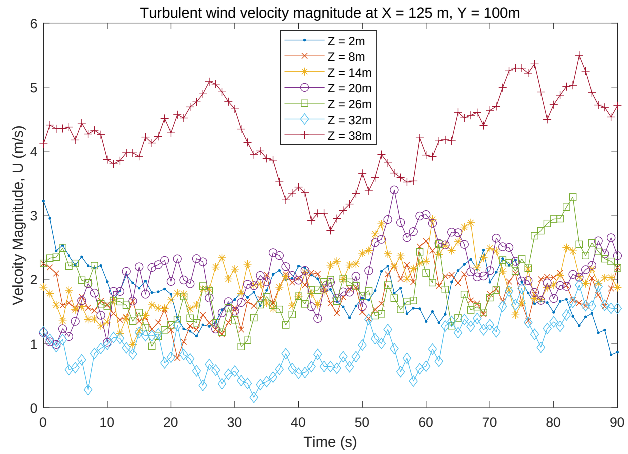

Figure 6. Time series of turbulent wind velocity data.

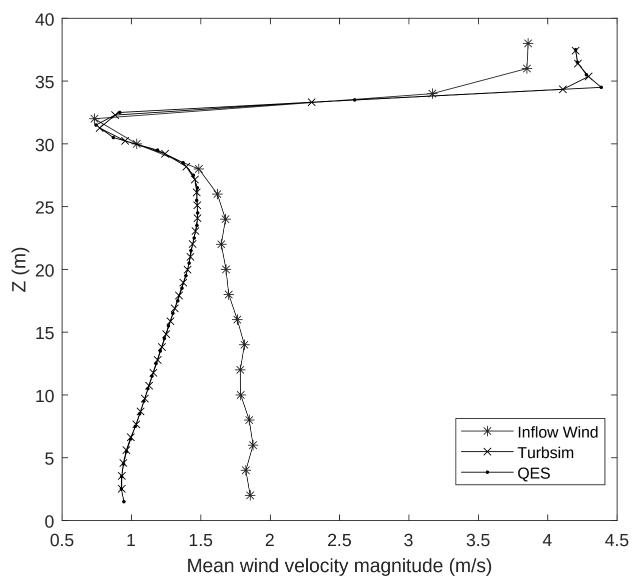

Figure 7. Mean wind velocity profile generated by QES, TurbSim, and InflowWind for a YZ plane at X=117 m.

performed with zero wind disturbance. Then, the same trajectory is traced and updated to account for the microscale wind disturbance, which is injected by querying the wind database consecutively at every 2 m altitude for each second of the flight time. Additionally, it is essential to also mention that both (with and without wind) the simulations are executed with the position hold feature of the controller switched on.

TRAJECTORY DEVIATION AND AIRCRAFT PERFORMANCE ANALYSIS

To adhere to the objective of this paper, the results from the flight simulations are assessed to distinguish the aircraft's response to wind disturbance only during landing.

From Fig. 11, it can be observed that the landing trajectory deviation is pronounced below 10 m altitude for the simulation with wind disturbance in comparison to the simulation with no wind disturbance as there is a lateral offset of about $\pm 2cm$. Likewise, there is also a lateral offset of 4 cm from the

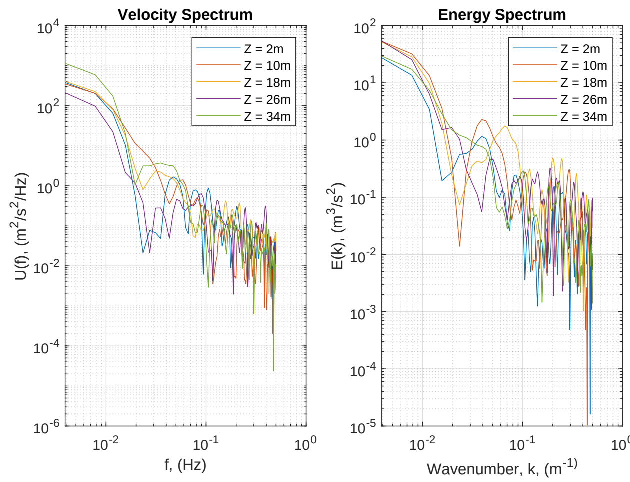

Figure 8. Turbulent velocity and energy spectrum at X=125 m, and Y=100 m.

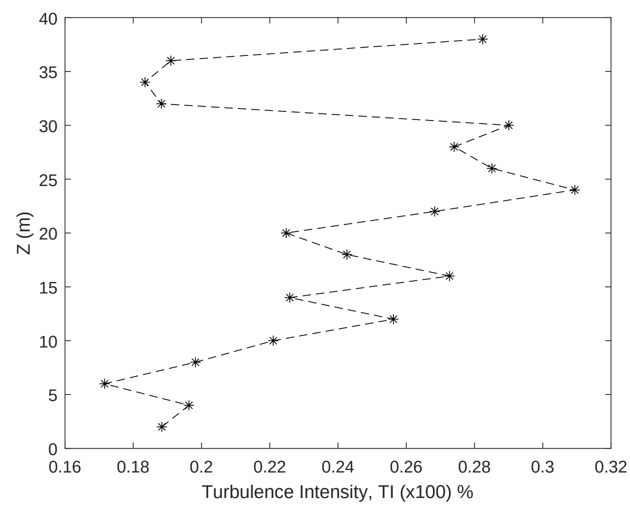

Figure 9. Turbulent intensity at X=125 m, Y=100 m.

setpoint trajectory at a 40 m altitude which could be owed to the performance of the multicopter mode controller during the transition from cruise to landing, as it is seen to be decreasing with altitude for no wind conditions.

Fig. 12 shows that there are minor fluctuations in the rate of change in vehicle airspeed indicating rapid swift in longitudinal and lateral velocity of aircraft within the first 5 seconds and last 10 seconds of the landing. This observation is in correlation with the deviation in the position of the aircraft observed in Fig. 11. Additionally, it can also be noticed that there are minute variations in the vertical deceleration at the initial and final seconds of the landing. This implies that the effects of vertical wind velocity are almost negligible on the aircraft landing trajectory and performance when compared to the lateral and longitudinal wind velocity.

For the rate of change of the roll, pitch and yaw angles of the aircraft with and without the presence of wind, it can be noticed in Fig. 13 that there are rapid oscillations of the aircraft below 7 m altitude or the final 10 seconds when compared

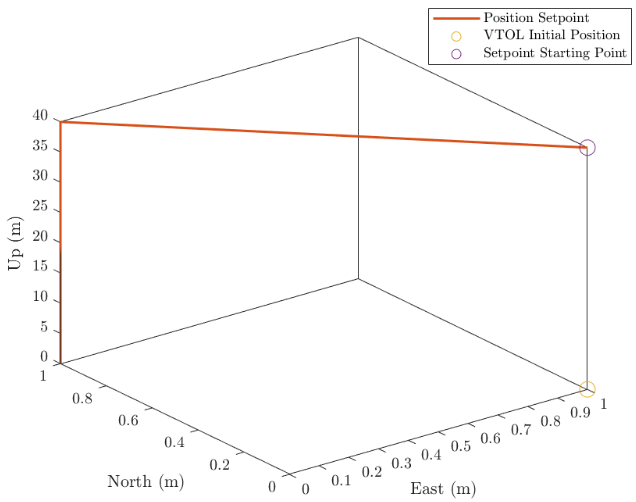

Figure 10. Setpoint trajectory.

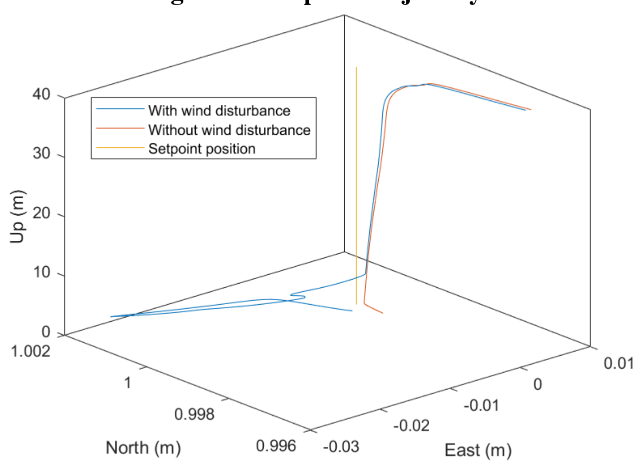

Figure 11. Landing trajectory with and without wind disturbance.

to the overall landing time. The roll angle and yaw angle deviate by $\pm 0.5deg$ and $-0.3deg$ and $+0.5deg$, respectively. Whereas, the pitch angle change is minimal at $\pm 0.05deg$. This further underscores that the wind velocity components, u and v have more effect on the aircraft response compared to the w or vertical component of the wind velocity.

In general, this analysis suggests that the controller in the loop rejects the wind disturbance sufficiently well and maintains the attitude and altitude of the aircraft to a larger extent during the landing phase. However, as the aircraft approaches closer to the ground, slight deviations can be observed in the lateral and longitudinal performance of the aircraft suggesting an increased influence of the u and v component of the turbulent wind velocities near the ground.

CONCLUSIONS

In summary, this paper investigates the effects of low-altitude microscale wind on the landing performance of an aircraft. Firstly, a test scenario is assumed to depict an eVTOL drone landing on the ground behind a building. Then, the microscale wind data is synthesized for the area over FATO and SA through the development of a novel wind modelling technique, which adopts highly parameterised steady state microscale wind simulator, QES-Winds and stochastic turbulent inflow wind generators, TurbSim and InflowWind. Later, the resultant 3D turbulent wind velocity data from the wind model is integrated with the eVTOL flight simulator. A simple trajectory is designed and traced with and without the presence of wind disturbances to differentiate the aircraft's landing performance from the wind.

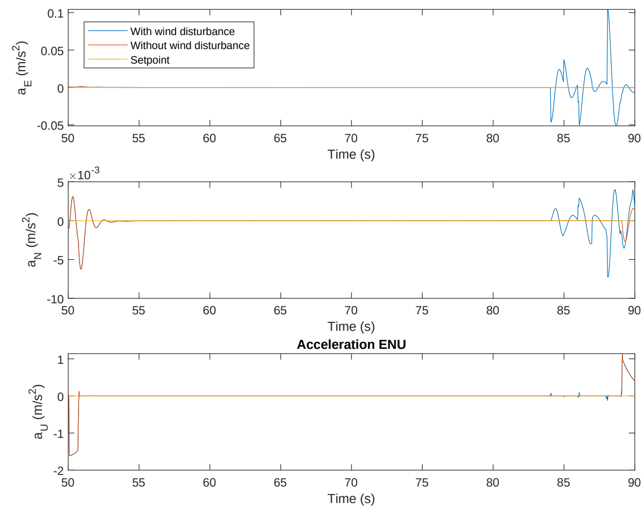

Figure 12. Acceleration with and without wind disturbance.

From the trajectory and aircraft performance analysis, it is evident that there is a slight deviation in the aircraft response to microscale wind disturbances when the vehicle is closer to the ground. The lateral and longitudinal variations in attitude are more pronounced compared to the vertical variations. This shows that the impact of streamwise, u, and lateral, v, wind velocity components is higher in comparison to the vertical, w, component of the wind velocity. Likewise, minor divergence is also observed in the first few seconds of the landing phase where the aircraft commences to decelerate from a hover. Overall, the results obtained from this analysis suggest that the controller maintains the attitude and altitude of the aircraft in the presence of wind disturbance fairly well within the FATO and SA.

However, it is essential to mention that the microscale wind data obtained through the wind modelling only describes the steady state wind velocity magnitude and the corresponding fluctuations within the assumed FATO and SA region. That is, the effects of wind angular rates, gust speeds and the corresponding change in aircraft angular rates and airspeed are not investigated. Moreover, as the wind data is not validated, the uncertainties pertaining to the wind modelling are still undetermined. Thus, the accuracy of the wind data is unknown at this point in time. Consequently, it is unclear whether the simulated wind data is representative of the low-altitude wind conditions in the real environment. Moreover, this also raises further repercussions within the aircraft performance analysis as the certainty of the aircraft response to the wind conditions

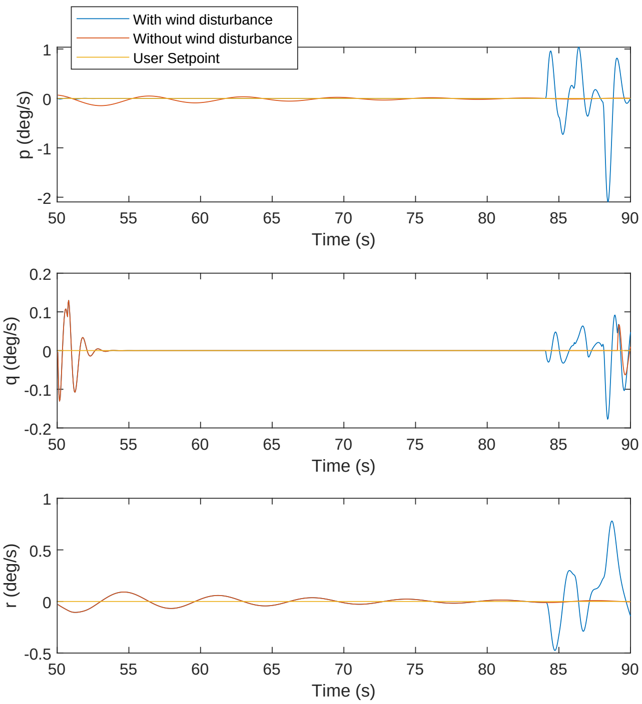

Figure 13. Rate of change of roll, yaw and pitch with and without wind disturbance.

becomes ambiguous. Along similar lines, another challenge encountered with wind modeling was the inability to reduce the grid size for the InflowWind propagation, as attempting to decrease the grid size resulted in output files larger than 15GB, which complicated post-processing data with MATLAB. Furthermore, the trajectory and aircraft performance analysis in this study does not specify the exact magnitude of the wind velocity responsible for the observed deviations.

Therefore, future works should include the following tasks:

1. Corroborate the wind data obtained from the wind model with wind tunnel or other experimental data to assess the wind model accuracy and associated uncertainty with the analysis.
2. Use of an optimized way to read large output files for data processing and analysis or reprogramming of the InflowWind output file structure and type.
3. Sensitivity analysis to determine how variations in wind velocity components affect the aircraft's performance, as this can aid in determining the probability and severity of deviation for different wind speeds, directions and intensity.

In conclusion, this paper presents a novel methodology for simulating and integrating microscale turbulent wind conditions for studying the effects of low-altitude wind on the performance of an eVTOL aircraft during near-ground flight phases. This approach serves as a simpler and more efficient alternative to microscale wind modelling for UAM applications when compared to the traditional CFD-based methods, the Von Kármán and Dryden gust models. Nevertheless, more work is required to refine and expand upon this methodology. Thus, the findings and recommendations from this study can serve as a foundation to further improve the microscale wind model and investigate the effects of low-altitude wind on the performance of eVTOLs for UAM aircraft testing and certification through simulation.

ACKNOWLEDGMENTS

This research is conducted under the REDI (RMIT European Doctoral Innovators) Program. This project has received funding from the European Union's Horizon 2020 research and innovation programme under the Marie Skłodowska-Curie grant agreement no. 101034328.

The authors would also like to thank the graduate student researchers at the ASCL laboratory at Politecnico di Milano, Italy for facilitating the flight simulator for this study.

REFERENCES

1. Zyadat, Z., Horri, N., Innocente, M., and Statheros, T., "Observer based optimal control of a quadplane with active wind disturbance and actuator fault rejection," *Sensors*, Vol. 23, (4), 2023, pp. –.
2. Pradeep, P., Chatterji, G. B., Sridhar, B., Edholm, K.-M., Lauderdale, T. A., Sheth, K., Lai, C. F., and Erzberger, H., "Wind-optimal trajectories for multirotor eVTOL aircraft on UAM missions," AIAA Aviation Forum, 2020.
3. Banerjee, P., Corbetta, M., Jarvis, K., Smalling, K., and Turner, A., "Probability of trajectory deviation of Unmanned aerial vehicle in presence of wind," *Journal of Air Transportation*, Vol. 31, 2023, pp. 128–139.
4. Taymourtash, N., Zagaglia, D., Zanotti, A., Muscarello, V., Gibertini, G., and Quaranta, G., "Experimental study of a helicopter model in shipboard operations," *Aerospace Science and Technology*, Vol. 115, 2021, pp. 106774.
5. Taymourtash, N., Zanotti, A., Gibertini, G., and Quaranta, G., "Unsteady load assessment of a scaled-helicopter model in a ship airwake," *Aerospace Science and Technology*, Vol. 129, 2022, pp. 107583.
6. Taymourtash, N., and Quaranta, G., "Turbulent Airwake Estimation from Helicopter–Ship Wind-Tunnel Data," *Journal of Aircraft*, 2024, pp. 1–10.
7. Taymourtash, N., *Experimental investigation of helicopter-ship dynamic interface*, Ph.D. thesis, Politecnico di Milano, Italy, 2021.
8. Bahr, M., Hebbar, U., Ferede, E., and Gandhi, F., "Multirotor eVTOL flight simulation and assessment under atmospheric turbulence," 77th Annual Forum & Technology Display, Vertical Flight Society, 2021.

9. Da Costa Siqueira, J. C., "Modeling of wind phenomena and analysis of their effects on UAV trajectory tracking performance," Technical report, West Virginia University, United States, 2017.

10. EASA, *Guidelines on Design verification for UAS operated in the 'specific' category, Issue 3*, European Union Aviation Safety Agency (EASA), Cologne, Germany, 2023.

11. EASA, *Special Condition for Light Unmanned Aircraft Systems — Medium Risk*, European Union Aviation Safety Agency (EASA), Cologne, Germany, 2020.

12. EASA, *Special Condition for small-category VTOL aircraft (SC-VTOL)*, European Union Aviation Safety Agency (EASA), Cologne, Germany, 2 July 2019.

13. Bozorgmehr, B., Patterson, Z., Willemsen, P., Margairaz, F., Gibbs, J., Stoll, R., and Pardyjak, E. R., "UtahEFD/QES-Public [Computer Software]," , June 2024.

14. Kelley, N., and Jonkman, B., "Overview of the TurbSim stochastic inflow turbulence simulator," Technical Report Version 1.21, National Renewable Energy Laboratory (NREL), Golden, CO, United States, 2007.

15. Platt, A., Jonkman, B., and Jonkman, J., "InflowWind User's Guide," Technical report, National Wind Technology Center (NWTC), National Renewable Energy Laboratory (NREL), United States, 2016.

16. Nithya, D. S., Quaranta, G., Muscarello, V., and Liang, M., "Review of Wind Flow Modelling in Urban Environments to Support the Development of Urban Air Mobility," *Drones*, Vol. 8(4), 2024, pp. 147.

17. Martello, N. C., "Modelling and integration of an eVTOL UAV," Technical report, Master Thesis, Politecnico di Milano, Italy, 2021.

18. Battaini, N., "Design and dynamic modeling of a VTOL UAV," Technical report, Master Thesis, Politecnico di Milano, Italy, 2019.

19. Martinelli, E., "Modelling, control, integration and testing of an eVTOL drone," Technical report, Master Thesis, Politecnico di Milano, Italy, 2022.

20. Willis, J. B., "Trajectory Generation and Tracking Control for Winged Electric Vertical Takeoff and Landing Aircraft," Technical report, Brigham Young University, Utah, United States, 2021.

21. EASA, *Third Publication of Means of Compliance with the Special Condition VTOL (MOC-3 SC-VTOL), Issue 2*, European Union Aviation Safety Agency (EASA), 21 June 2023.